*ally heterogeneous materials*: Syn. of Thesis for Dr. of Techn. Sci. Degree. Tomsk.
2. Karzov, G.P., Margolin, B.Z., Shvetsova, V.A. (1993) *Physical-mechanical modeling of fracture processes*. St.-Petersburg: Politekhnika.
3. Rybin, V.V. (1986) *High plastic strains and fracture of metals*. Moscow: Metallurgiya.
4. (1986) *Static strength and fracture mechanics of steels*. Ed. by V. Dal, V. Antonov. Moscow: Metallurgizdat.
5. Makhnenko, V.I. (1976) *Computational methods for investigation of kinetics of welding stresses and strains*. Kiev: Naukova Dumka.
6. Makhnenko, V.I., Velikoivanenko, O.A., Pozynka, G.P. et al. (2009) Stressed state in zone of thinning defects of thin-wall pipes. In: *Problems of service life and service safety of structures, buildings and machines*. Ed. by B.E. Paton. Kyiv: PWI.
7. (2000) *Fitness-for-service*: American Petroleum Institute recommended practice 579. 1st ed.

# INFLUENCE OF WELDING THERMAL CYCLE ON STRUCTURE AND PROPERTIES OF MICROALLOYED STRUCTURAL STEELS

**V.A. KOSTIN, G.M. GRIGORENKO, V.D. POZNYAKOV, S.L. ZHDANOV, T.G. SOLOMIJCHUK, T.A. ZUBER** and **A.A. MAKSIMENKO**
E.O. Paton Electric Welding Institute, NASU, Kiev, Ukraine

Influence of welding thermal cycle on microstructure and properties of HAZ metal in new steels with carbide and carbonitride type of strengthening, namely 06GBD, 10G2FB, 15KSATYuD, was studied. It is shown that under the influence of welding thermal cycle an optimum complex of ferritic-bainitic structures forms in a rather broad range of cooling rates ($w_{6/5}$ = 10–30 °C/s), which is characterized by values of strength, ductility and cold resistance on the level of requirements made of base metal of strength class C440.

***Keywords:*** *arc welding, structural steels, carbonitride strengthening, welding thermal cycle, Gleeble 3800, microstructure, bainite, MAC-phase, mechanical properties*

At present transportation engineering and building industry of Ukraine are the main users of higher strength steels with yield point of up to 400 MPa. Today, however, they no longer satisfy, by a number of objective factors, the requirements of high-speed traffic or modern concepts of urban planning, both by the level of strength and impact toughness.

Over the recent years, PWI in cooperation with metallurgists developed a number of new steels with 440–590 MPa yield point, based on the principle of carbide and carbonitride strengthening [1, 2].

As welding is the main technological process of fabrication of structures from these steels, improved performance of the new steels (by strength and impact toughness level) should be preserved also in the welded joints. However, HAZ formation in the metal being welded leads to deterioration of mechanical properties under the impact of welding thermal cycle (WTC), both as a result of grain growth, and in connection with formation of quenching structures. Wide introduction of new steels should be preceded by profound comprehensive investigation of these steels reaction to WTC.

Disembodied published data on the features of structural changes in the new steels with carbide and carbonitride strengthening under WTC conditions are obviously insufficient [3, 4].

In addition, the clearly increased requirements to impact toughness of new steels of strength class C345–440 ($KCU_{-40}$ = 39 J/cm$^2$, $KCU_{-70}$ = 34 J/cm$^2$ to GOST 27772–88) require studying WTC effect on strength and impact toughness levels in HAZ metal.

The objective of this work consisted in investigation of the features of formation of HAZ metal structure under WTC impact and assessment of microstructure influence on mechanical properties and impact toughness in this zone, in order to select optimum welding modes, ensuring high performance of the welded joint.

Table 1 gives the composition of the studied steel grades. Steels 10G2FB and 06GBD belong to steels with carbide strengthening type, and 15KhSATYuD steel is of carbonitride strengthening type. Mechanical properties of steels in as-delivered condition are given in Tables 2 and 3.

In order to evaluate WTC effect on the structure of welded joint HAZ metal, investigations were conducted on model samples in Geeble 3800

**Table 1.** Composition of studied steels, wt.%

| Steel grade | C | Si | Mn | Cr | Ti | Nb |
|---|---|---|---|---|---|---|
| 15KhSATYuD (δ = 12 mm, strength class C345 to GOST 27772–88) | 0.145 | 1.12 | 0.76 | 0.56 | 0.03 | – |
| 10G2FB (δ = 18.7 mm, strength class K60 to TU 1381-009-47966425–2007) | 0.079 | 0.25 | 1.57 | 0.04 | – | 0.05 |
| 06GBD (δ = 20 mm, strength class C390 to TU U 27.1-05416923-085:2006) | 0.066 | 0.19 | 1.23 | 0.22 | – | 0.03 |

**Table 1** (cont.)

| Steel grade | Mo | Cu | V | Al | N | S | P |
|---|---|---|---|---|---|---|---|
| 15KhSATYuD (δ = 12 mm, strength class C345 to GOST 27772–88) | – | 0.31 | – | 0.041 | 0.015 | 0.029 | 0.026 |
| 10G2FB (δ = 18.7 mm, strength class K60 to TU 1381-009-47966425–2007) | 0.19 | ≤0.02 | 0.05 | 0.032 | 0.006 | 0.007 | 0.013 |
| 06GBD (δ = 20 mm, strength class C390 to TU U 27.1-05416923-085:2006) | 0.13 | 0.22 | – | – | 0.006 | 0.009 | 0.010 |

system for simulation of welding thermodeformational cycle. For this purpose samples of 6 mm diameter and 86 mm length were heated in a high-speed dilatometer up to the temperature of 1350 °C at the rate of 150 °C/s. After that they were cooled in keeping with the specified thermal cycles, characteristic for basic modes of arc welding of the studied steels at rate $w_{6/5}$ varying from 1 up to 60 °C/s. Dylatometric study results were used to plot diagrams of decomposition of austenite in the studied steels (Figure 1). WTC effect on mechanical properties and impact toughness of the studied steels was assessed by heat treatment of model samples in MSR-75 unit by a procedure developed at PWI [5].

Processing of the results of dylatometric analysis and diagram plotting were performed by the common procedure. Calculation of the ratio of transformation products was conducted by dylatometric curves, using segment approach [6].

Metallographic investigations were conducted using light microscope «Neophot-32». Microstructure was revealed by etching in nital (4 % solution of nitric acid in alcohol). Hardness was measured by Vickers at 50 N load. Structural constituents were calculated by field method to GOST 8233–56.

Microstructural analysis showed that 15KhSATYuD steel in the initial condition has ferritic-pearlitic structure of various dispersity, with varying amount of pearlite and pronounced striation (Figure 2, *a*). Grain size corresponds to point 4 (71–97 μm). Metal of this steel contains a large quantity of nonmetallic inclusions, predominantly manganese sulphides, which are located in ferrite regions.

**Table 2.** Mechanical properties of studied steels

| Steel grade | Along rolling direction | | | | Across rolling direction | | | |
|---|---|---|---|---|---|---|---|---|
| | $\sigma_y$, MPa | $\sigma_t$, MPa | $\delta_5$, % | ψ, % | $\sigma_y$, MPa | $\sigma_t$, MPa | $\delta_5$, % | ψ, % |
| 15KhSATYuD | 411 | 564 | 33.1 | 64.5 | 407 | 560 | 30.7 | 52.4 |
| 10G2FB | 576 | 660 | 25.1 | 62.3 | 521 | 608 | 25.4 | 64.8 |
| 06GBD | 400 | 578 | 30 | 84 | – | – | – | – |

**Table 3.** Results of impact bend testing of studied steels

| Steel grade | Rolling direction | *KCU*, J/cm$^2$, at temperature, °C | | | *KCV*, J/cm$^2$, at temperature, °C | | |
|---|---|---|---|---|---|---|---|
| | | 20 | –40 | –60 | 20 | –40 | –60 |
| 15KhSATYuD | Along | 120 | 72 | 65 | 84 | 26 | 14 |
| | Across | 82 | 44 | 40 | 46 | 25 | 15 |
| 10G2FB | Along | 346 | 347 | 324 | 344 | 346 | 345 |
| | Across | 345 | 279 | 220 | 323 | 256 | 204 |
| 06GBD | Along | 348 | 348 | – | 349 | 317 | – |

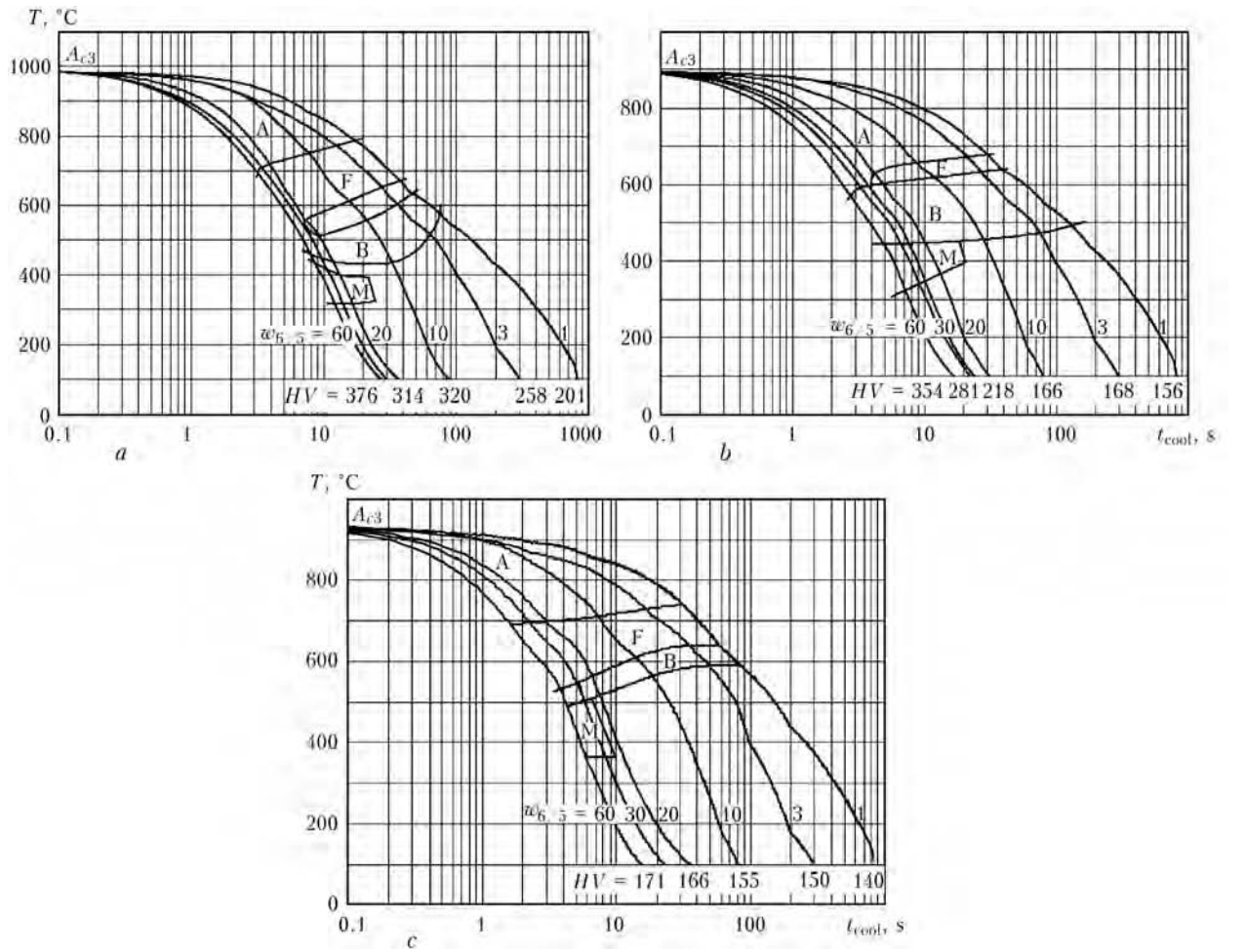


**Figure 1.** Thermokinetic diagram of austenite decomposition in steels with carbonitride strengthening: *a* — 15KhSATYuD; *b* — 10G2FB; *c* — 06GBD

Microstructure of samples of 10G2FB steel in as-delivered condition is ferritic-bainitic with a small amount of pearlite, obtained as a result of application of rolling stock thermostrengthening technology. Structure consists of sections of polygonal ferrite, tempered bainite and finely-dispersed pearlite (Figure 2, *b*). Grain point is 4–5. Steel 10G2FB is characterized by rolling stock texture and stringer anisometry.

Mictrostructure of samples of 06GBD steel is a finely-dispersed ferritic-pearlitic structure with grain size of 5–15 μm (Figure 2, *c*). A certain anisometry of ferrite grains is found, the dimensions of which correspond to point 4–6 (40–80 μm). Finely-dispersed pearlite is observed in the form of individual isolated sections along the boundaries and at the junction of ferrite grains. A small amount of carbon (0.06 %) and observed differences in pearlite colour allow assuming that individual sections (of lighter colour) are those of martensite-austenite-carbide complexes (MAC-phases). Rolling texture is completely absent from the structure.

Toughness of steels with carbonitride strengthening in as-delivered condition was evaluated on standard sample with U- and V-


**Figure 2.** Microstructures (×500) of studied steels: *a* — 15KhSATYuD; *b* — 10G2FB; *c* — 06GBD

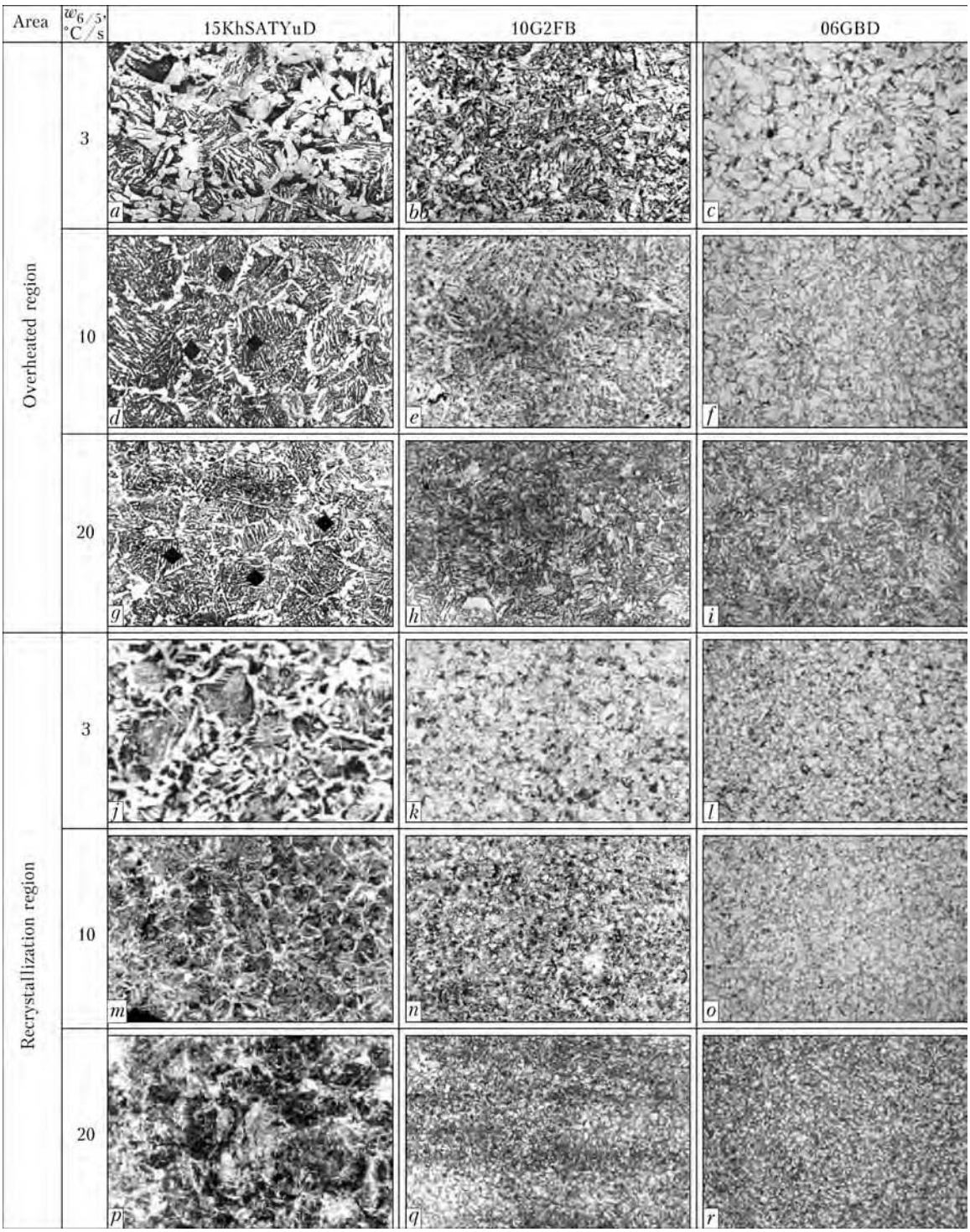


**Figure 3.** Influence of cooling rate on microstructure (×500) of simulated sections of HAZ metal in overheating and recrystallization zones (for *a*–*r* see the text)

shaped notch for impact bending according to GOST 9454–78. Obtained results are indicative of the fact that in 10G2FB and 06GBD steels toughness margin is much higher than in 15KhSATYuD steel, and brittle transition temperature is below –60 °C (Table 3).

Metallographic analysis of simulation samples of overheating zone from 15KhSATYuD steel showed that austenite transformation at their continuous cooling at the rate of 3 °C/s occurs in the ferritic, pearlitic and bainitic regions. Therefore, this steel structure contains quite a lot of ferrite (Figure 3, *a*). Hypoeutectoid ferrite of polygonal morphology precipitated along austenite grain boundaries, and sections of pealite precipitates are observed at the junction of ferrite grains and inside them. Widmanstatten ferrite is found locally. Inside the austenite grains of these steels the structure was identified as globular bainite. These structural changes lead

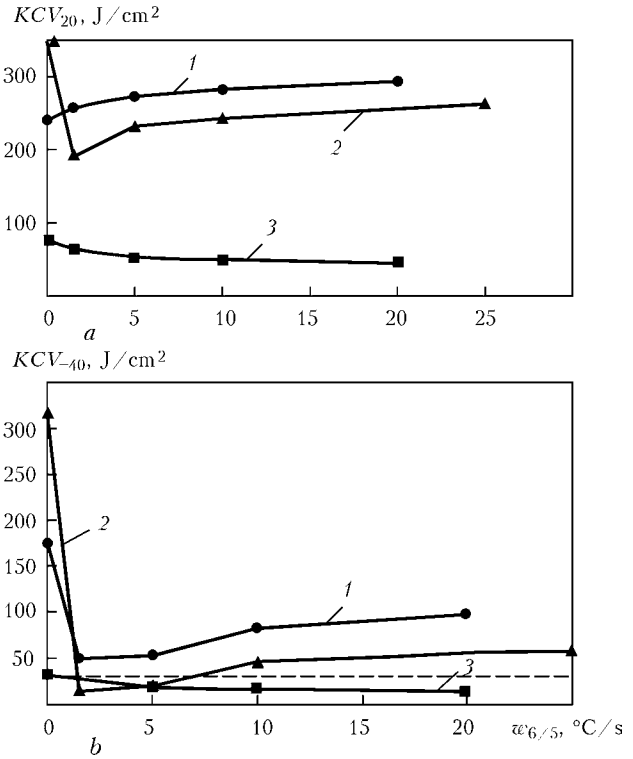


**Figure 4.** Dependence of impact toughness values *KCV* of HAZ metal on its cooling rate $w_{6/5}$ at 20 (*a*) and –40 (*b*) °C: *1* — 06GBD; *2* — 10G2FB; *3* — 15KhSATYuD (dash line — strength class C440)

to a monotonic lowering of ductility and impact toughness values at temperature below 0 °C.

The most coarse-grained structure formed in samples of 10G2FB steel at cooling at the rate of 3 °C/s (Figure 3, *b*). Hypoeutectoid polygonal

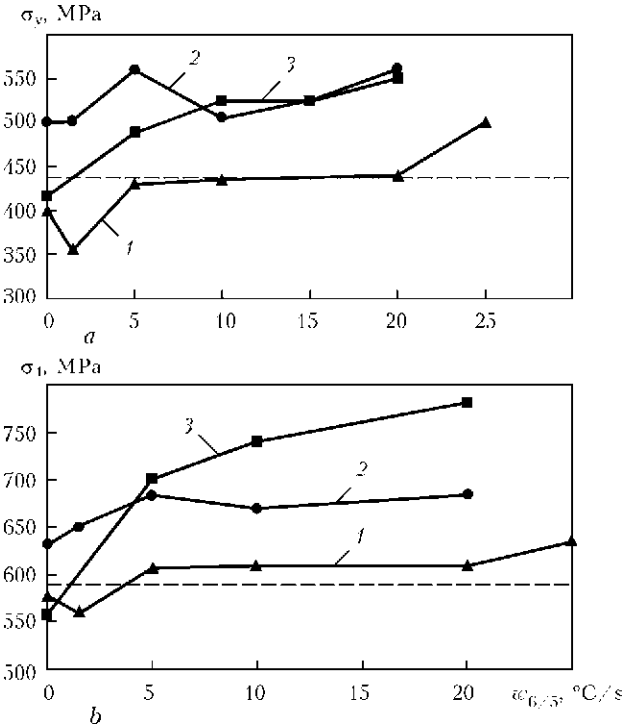


**Figure 5.** Dependence of strength properties ($\sigma_y$ and $\sigma_t$) of HAZ metal on its cooling rate (designations are the same as in Figure 4)

ferrite and pearlite precipitate along the grain boundaries, and bainite of two morphological varieties: high-temperature (low-carbon) with microhardness of 1850–2030 MPa and low-temperature with microhardness of 2140–2430 MPa forms inside the grains. Such a structural change leads to an abrupt drop of HAZ metal cold resistance at temperature of –20 °C and lower (Figure 4), as well as increase of strength values (Figure 5) and lowering of values of relative elongation with a slight increase of values of reduction-in-area (Figure 6).

In 06GBD steel an anisometric ferritic-bainitic structure is found at cooling at the rate of 3 °C/s (Figure 3, *c*). Bainite formation occurs in the sections with higher carbon content (former pearlite grain regions). Relatively coarse ferrite grains (point 8, about 20–22 μm) along the boundaries are surrounded by uniformly distributed finer bainitic grains (point 10, 10 μm). Bainite microhardness is equal to about 1820–1890 MPa.

With increase of cooling rate to 10° C/s the conditions for austenite homogenizing process become less favourable than at $w_{6/5}$ = 3 °C/s. In this connection in the structure of 15KhSATYuD steel the quantity of bainitic component rises abruptly, and quantity of structurally-free bainite and pearlite decreases abruptly (Figure 3, *d*, *m*), thus leading to higher values of HAZ metal strength and lowering of its ductility properties.

Structurally-free hypoeutectoid ferrite precipitates as a net along austenite grain bounda-

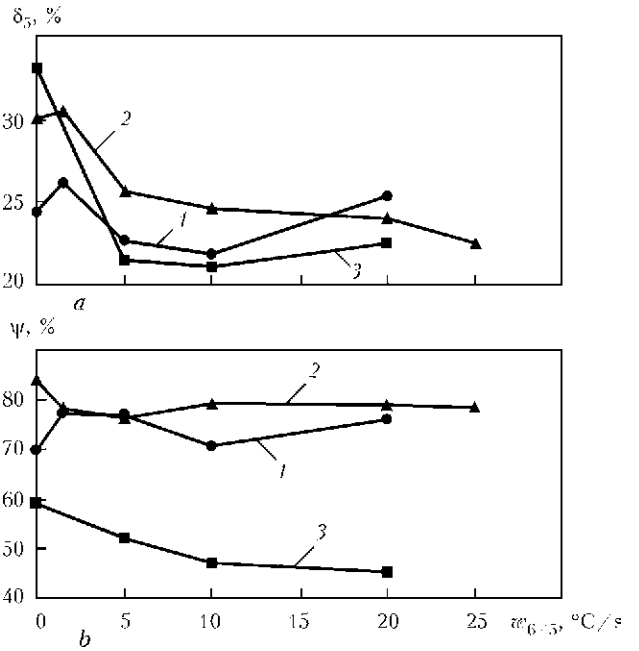


**Figure 6.** Dependence of ductility properties ($\delta_5$ and $\psi$) of HAZ metal on its cooling rate (designations are the same as in Figure 4)

ries, whereas pearlite is sometimes found near ferrite grains. Bainite was identified as granular. Size of bainite grains at cooling rate $w_{6/5}$ = = 3 °C/s practically did not change.

Results of metallographic analysis of microstructure of simulation samples from steel 15KhSATYuD, formed at $w_{6/5}$ = 10 °C/s, are indicative of the fact that austenite overcooling becomes greater at increase of cooling rate that results in an increase of its resistance and lowering of transformation temperature of both ferrite from 800 to 750 °C, and bainite from 630 to 550 °C. Amount of bainitic constituent rises. Increase of the amount of bainite in the structure causes an increase of hardness in the complete recrystallization region, as well as of strength values. At the same time, ductility and impact toughness values (Figure 4) decrease.

Cooling of 10G2FB steel at the rate of 10 °C/s leads to narrowing of the region with overheated structure and grain refinement. Compared to cooling rate of 3 °C/s, structural changes in this case promote a reduction of the amount of hypoeutectoid polygonal ferrite and low-carbon bainite, and increase of the amount of high-carbon bainite (Figure 3, *e*, *n*). Pearlitic transformation at this rate is almost completely absent. Temperatures of ferrite and bainite transformation decrease to a smaller degree than in 15KhSATYuD steel. Such a nature of microstructure leads to a small increase of impact toughness values (see Figure 4), values of strength and reduction in area are on base metal level (Figures 5 and 6), whereas values of relative elongation decreased to 21 % (Figure 6).

Results of metallographic analysis of 06GBD steel formed at $w_{6/5}$ = 10 °C/s show that it consists of ferrite, bainite and small regions of MAC-phase precipitates (about 1 %, Table 4).

Bainite grains are observed in the form of elongated plates of upper bainite, formed both along ferrite grain boundaries, and of preserved equiaxed regions of granular bainite (Figure 3, *f*, *o*) With increase of cooling rate to $w_{6/5}$ = = 10 °C/s, microhardness of bainitic structure rises up to 2190 MPa, mainly due to increase of the quantity of its high-temperature species. MAC-phase distribution in the structure is uniform. Change of phase transformation temperature turns out to be negligible (lowering by approximately 20–30 °C).

Analysis of microstructure of simulation samples from 15KhSATYuD steel formed as a result of cooling at the rate of $w_{6/5}$ = 20 °C/s (Figure 3, *g*, *p*) showed a complex combination of bainite of granular and plate-like morphology,

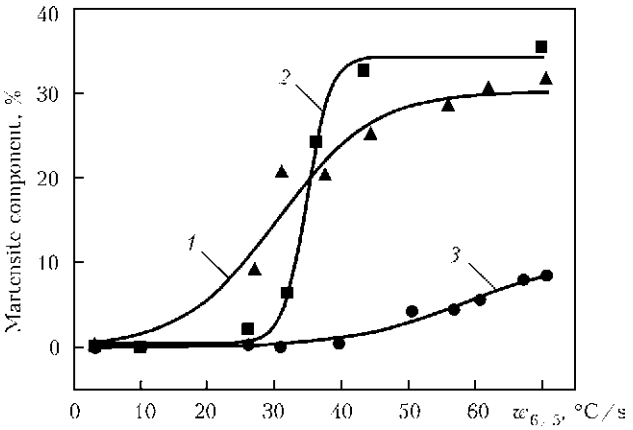


**Figure 7.** Influence of cooling rate on fraction of martensite component in the studied steels: *1* — 15KhSATYuD; *2* — 10G2FB; *3* — 06GBD

as well as hypoeutectoid ferrite and a small quantity of acicular ferrite. Bainite microhardness changes from 2150–2200 (for granular bainite) to 1930–1980 MPa (for plate-like bainite).

Microstructure of samples from steel 10G2FB formed as a result of cooling at the rate of $w_{6/5}$ = = 20 °C/s revealed further narrowing of the region simulating the overheating zone, at reduction of grain size. In the simulated region structure hypoeutectoid polygonal ferrite is seldom found along grain boundaries. Main components of such metal structure are low-temperature bainite (granular, with microhardness of 2100 to 2360 MPa) and to a smaller extent — high-temperature bainite (1850–2030 MPa) (Figure 3, *h*, *q*). Values of strength, ductility and cold resistance almost did not change.

Cooling of 06GBD steel at the rate of $w_{6/5}$ = = 20 °C/s leads to further increase of the amount of products of intermediate transformation (bainite and MAC-phases, Table 4). Microhardness of bainitic component rises up to 2220–2390 MPa (Figure 3, *i*, *r*). Strength and impact toughness values in 06GBD steel remain on the level of 10G2FB steel.

Further increase of cooling rate (above 30 °C/s) in 15KhSATYuD and 10G2FB steels leads to formation and increase of the fraction of martensite component in the total complex of microstructures (Figure 7) that abruptly lowers their impact toughness and ductility values. In 06GBD steel the martensite component practi-

**Table 4.** Fraction of structural constituents in 06GBD steel at different cooling rates, %

| Cooling rate, °C/s | Ferrite | Bainite | MAC-phase |
|---|---|---|---|
| 3 | 94.10 | 5.90 | – |
| 10 | 79.29 | 19.51 | 1.20 |
| 20 | 68.09 | 27.76 | 4.15 |

cally does not form, because of low carbon content (0.06 %) that is in good agreement with mechanical testing results.

Comparison of mechanical testing results of samples, simulating the HAZ of the studied steels (see Figures 4–6) shows that increase of cooling rate leads to gradual increase of yield point and strength, as well as ductility lowering due to increase of martensitic component. WTC has the greatest effect on impact toughness at below zero temperatures (see Figure 4, *b*). In 10G2FB steel $KCV_{-40}$ impact toughness decreases from 320 to 25 J/cm$^2$, in 06GDB steel — from 170 to 50 J/cm$^2$, and in 15KhSATYuD steel — from 46 to 22 J/cm$^2$ already at the cooling rate of 1 °C/s. Such an abrupt drop of toughness of steels with carbide strengthening can be associated with partial dissolution of the carbide phases during WTC [7]. At further increase of cooling rate from 1 up to 30 °C/s, sample toughness slightly rises due to a change in bainitic structure morphology from plate-like to granular one.

At impact bend testing of standard samples with U-shaped notch all the studied steel demonstrated a good toughness ($KCU_{-40} \geq$ $\geq$ 50 J/cm$^2$). At impact bend testing of standard samples with a sharp V-shaped notch impact properties at below zero temperatures (to –40 °C) correspond to the requirements of GOST 27772–88 for steels of strength class C345–440 only for steels with carbide strengthening 10G2FB and 06GBD at cooling rates of 10–25 °C/s.

Impact toughness of simulation samples of 15KhSATYuD steel with a sharp notch $KCU_{-40}$ at cooling rate of 10 °C/s is equal to 20 J/cm$^2$, and at 25 °C/s it is only 12 J/cm$^2$ that is related to the features of arrangement of carbonitride particles during secondary precipitation [8]. Investigations reveal the need for correction of the composition of 15KhSATYuD steel, in order to improve its toughness at WTC impact.

Results of these investigations were a scientific basis for application of new 06GBD steel in construction of a motor road bridge across the entrance to the Bay of Podol Bridge Crossing in Kiev [9] and application steel of 10G2FB type in the arch structure of the roofing of a new stadium in Kazan (Russia).

## CONCLUSIONS

1. Under the conditions of WTC simulation at cooling rates of 1–60 °C/s, austenite transformation in the studied steels 15KhSATYuD, 10G2FB and 06GBD occurs in the ferritic, bainitic and martensitic regions.

2. At impact bend testing of standard samples with U-shaped notch all the studied steels 15KhSATYuD, 10G2FB and 06GBD demonstrated high performance (according to GOST $KCU_{-60} > 29.4$ J/cm$^2$). At testing of standard samples with a sharp V-shaped notch only steels 10G2FB and 06GBD with carbide strengthening at cooling rates up to 1 and 10–25 °C/s correspond to the requirements (according to GOST $KCU_{-40} > 39$ J/cm$^2$).

3. Optimum values of mechanical properties and impact toughness in samples of steels 10G2FB and 06GBD are achieved due to formation of a ferritic-bainitic structure in them at cooling rates of 10–25 °C/s with a small amount of brittle martensitic phase.


1. Matrosov, Yu.I., Litvinenko, D.A., Golovanenko, S.A. (1989) *Steel for main pipelines*. Moscow: Metallurgiya.
2. Shipitsyn, S.Ya., Babaskin, Yu.Z., Kirchu, I.F. et al. (2008) Microalloyed steel for railway wheels. *Stal*, **9**, 76–79.
3. Gretsky, Yu.Ya., Demchenko, Yu.V., Vasiliev, V.G. (1993) Formation of HAZ metal structure of low-silicon steel with carbonitride strengthening. *Avtomatich. Svarka*, **9**, 3–5, 22.
4. Zakharova, I.V., Chichkarev, E.A., Vasiliev, V.G. et al. (2001) Structure and properties of HAZ metal of low-alloyed pipe steels modified with calcium. *The Paton Welding J.*, **8**, 14–17.
5. Sarzhevsky, V.A., Sazonov, V.Ya. (1981) Unit for simulation of welding thermal cycles on the base of MSR-75 machine. *Avtomatich. Svarka*, **5**, 69–70.
6. Steven, W., Mayer, G. (1953) Continuous-cooling transformation diagrams of steels. Pt 1. *J. Iron and Steel Institute*, **174**, 33–45.
7. Livshits, L.S. (1979) *Metals science for welders (welding of steels)*. Moscow: Mashinostroenie.
8. Zmienko, D.S., Stepanova, I.A., Yaropolova, E.I. et al. (2008) Identification of nanoparticles of niobium carbide in steel 10Kh13G12S2N2D2B. *Zavod. Laboratoriya. Diagn. Mater.*, 74(**6**), 40–42.
9. Sineok, O.G., Gerasimenko, A.M., Ryabokon, V.D. et al. (2010) Application of current welding consumables and technologies for welding of improved strength rolled metal. *Visnyk Dnipropetr. Nats. Untu Zalizn. Transporty im. Akad. V. Lazaryana*, Issue 33, 245–250.